

Electron spin lattice relaxation in some metal dithiolene matrices with $^{63}\text{Cu}(\text{II})$ centres

PERIAKARUPPAN T MANOHARAN^{1*}, J SHEILA ANNIE¹ and SUSANNE PFENNINGER²⁺

¹Department of Chemistry, Indian Institute of Technology, Madras 600 036, India

²Laboratorium Für Physikalische Chemie, Eidgenössische, Technische Hochschule, CH 8092 Zürich, Switzerland

+Present address: Institute für Physikalische Chemie, Universität Basel, CH-4056 Basel, Switzerland

Abstract. Temperature dependence of the electron spin-lattice relaxation time T_1 , of ^{63}Cu doped metal dithiolene matrices were studied by continuous wave and time-domain EPR methods. Measurements were made in the temperature range from 10–300 K for $(n\text{-Bu}_4\text{N})_2\text{Pt}(\text{dtsq})$, $(n\text{-Bu}_4\text{N})_2\text{Pt}(\text{dcmdtcroc})_2$, $(n\text{-Bu}_4\text{N})_2\text{Pd}(\text{dtcroc})_2$ and $(n\text{-Bu}_4\text{N})_2\text{Ni}(\text{mnt})_2$ matrices where (dtsq) is dithiosquarate, (dcmdtcroc) is dicyanomethylenedithiocrocanate, (dtcroc) is dithiocrocanate and (mnt) is maleonitriledithiolate. In all systems T_1 seems to be of the order of a few μs above 80 K. In $(n\text{-Bu}_4\text{N})_2[^{63}\text{Cu}/\text{Pt}(\text{dcmdtroc})_2]$, the T_1 values have been found to vary between 0.52 and 770 μs between 300 K and 20 K, respectively. The temperature dependence of the electron spin-lattice relaxation rate is about T^{-3} . Temperature-dependent T_1 values thus obtained have been interpreted in terms of both direct and Raman processes.

Keywords. Electron spin-lattice relaxation; cw and pulse methods; direct and Raman processes.

1. Introduction

The dominant electron spin-lattice interaction of paramagnetic ions in crystals, characterized by the time T_1 , have been shown earlier to occur through thermal modulation of crystalline electric field (Schlick and Kevan 1976). The relaxation processes such as direct (one phonon) and Raman (involving two phonons) are temperature dependent. The common methods to measure the spin-lattice relaxation time are power saturation, which is a continuous wave (cw) EPR method, or pulsed methods such as saturation or inversion recovery. These methods have been performed on iron and cupric ions among the first row transition ions and a series of rare earth ions. Among them, some of the most interesting and remarkable studies have been performed using single crystals (Attanasio *et al* 1976; Schlick and Kevan 1976; Kirmse *et al* 1978, 1980, 1982; Stach *et al* 1978, 1979, 1984; Keijzers and Snaathorst 1980; Snaathorst *et al* 1980; Mabbs and Temperly 1989; Sheila Annie and Manoharan 1992) and biomolecules (Brudwig *et al* 1984; Scholes *et al* 1984; Drews *et al* 1990) such as cytochrome C-oxidase and blue-copper proteins. In some crystalline materials the observation of spin-flip transitions permits differential saturation of the two EPR

*For correspondence

lines – main and satellite (Schlick and Kevan 1976; Sheila Annie and Manoharan 1992) – because they are controlled by different spin-lattice relaxation mechanisms and transition probabilities. It should also be noted that in a large number of lattices the EPR lines were broadened to different extents due to the presence of unresolved hyperfine interactions with the neighbouring ligands making it sometimes difficult to interpret the temperature-dependence of T_1 . Most metal dithiolenes do not contain nearby magnetic nuclei and therefore are ideal molecules for such studies.

The EPR spectra of diluted paramagnetic metal dithiolenes are characterized by linewidths of about 0.25 to 0.4 mT that permit the observation of spin-flip transitions (Attanasio *et al* 1976; Kirmse *et al* 1978, 1980, 1982; Stach *et al* 1978, 1979, 1984; Keijzers and Snaathorst 1980; Snaathorst *et al* 1980; Mabbs and Temperly 1989) from far-off protons appearing as satellites on either side of the metal hyperfine main lines, mainly due to the absence of any nearby magnetic nuclei. Kirmse *et al* (1980) have explained the small EPR line widths observed in these complexes from T_1 data. The analysis of spin-flip transition in ^{63}Cu -doped dithiolenes (Sheila Annie and Manoharan 1992) revealed that the differential saturation behaviour of the Cu hyperfine lines and the spin-flip satellites at low temperatures could give useful information on the relaxation mechanisms operating in the studied systems. Here, we report the temperature dependence of T_1 between 20 and 300 K for the following ^{63}Cu -doped metal dithiolene matrices. (a) $(n\text{-Bu}_4\text{N})_2 \text{Pt}(\text{dtsq})_2$, (b) $(n\text{-Bu}_4\text{N})_2 \text{Pt}(\text{dcm dtcroc})_2$, (c) $(n\text{-Bu}_4\text{N})_2 \text{Pd}(\text{dtcroc})_2$, (d) $(n\text{-Bu}_4\text{N})_2 \text{Ni}(\text{mnt})_2$, where the ligands are: dtsq – dithiosquarate, dcm dtcroc – dicyanomethylene-dithiocrocanate, dtcroc – dithiocrocanate and mnt – maleonitriledithiolate. The molecular structures of these almost rigorously dithiolene matrices are shown in figure 1. The coordinate system is also shown in figure 1 where the molecular x-axis is along the bisector of a single dithiolene ligand, the y-axis between two bidentate ligands and the z-axis perpendicular to the molecular plane.

Our earlier report (Sheila Annie and Manoharan 1992) on these systems was limited to the study of the relative intensities of satellite (due to spin flip transitions) vs main (hyperfine line due to ^{63}Cu) EPR lines. It was found by power saturation studies at temperatures around 77 K and above that (i) there was an increase in the intensity of satellite lines with increase in microwave power with no apparent saturation at room temperature, while the main lines saturated at higher power levels; (ii) a study of T_1 (satellite)/ T_1 (main) as a function of temperature revealed that the experimental T_1 ratios at high temperature and low temperature regions depended on different relaxation processes (Shimuzu 1965; Schlick and Kevan 1976; Sheila Annie and Manoharan 1992); (iii) lowering the temperature at a constant but low microwave power level has the same effect as that of increasing the microwave power; (iv) T_1 was found to substantially increase below 100 K in all compounds. In general, T_1 values measured with cw methods are effective values whereas with pulsed methods intrinsic T_1 's are measured. Continuous wave methods cannot separate or cancel different T_1 influencing processes. Therefore, T_1 has been mainly measured by inversion recovery. We have only been able to measure T_1 of the mainline with pulsed technique because of the small intensity of the satellites in pulsed EPR. In the following we present T_1 values at different temperatures measured either by saturation or pulsed methods. It allows us to draw some important conclusions on relaxation processes and temperature-dependence of T_1 at low temperature.

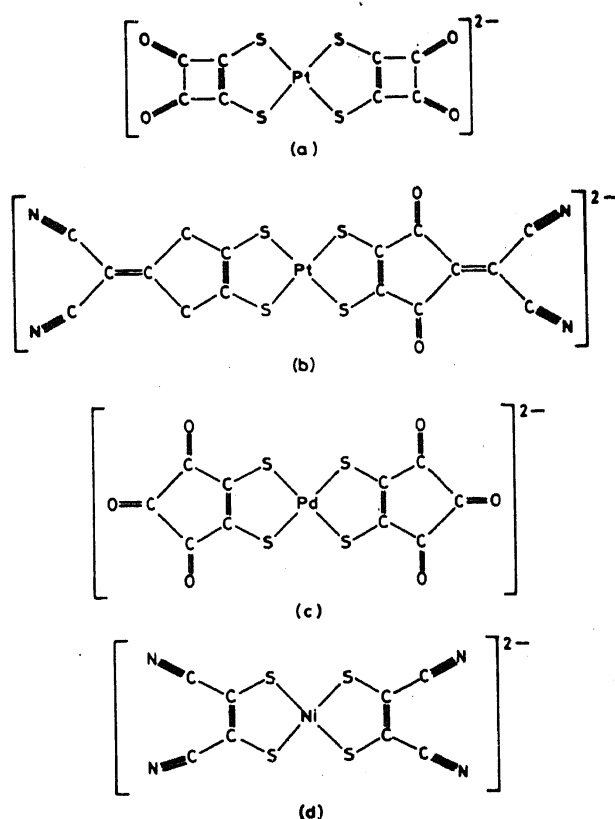


Figure 1. Molecular structures of (a) $[\text{Pt}(\text{dtsq})_2]^{2-}$, (b) $[\text{Pt}(\text{dcmdtroc})_2]^{2-}$, (c) $[\text{Pt}(\text{dtroc})_2]^{2-}$ and (d) $[\text{Ni}(\text{mnt})_2]^{2-}$.

2. Materials and methods

2.1 Preparation of samples

The diamagnetic host lattices of Pt, Pd and Ni dithiolenes and the corresponding ^{63}Cu paramagnetic complexes were made by known literature methods (Bahr and Schleiter 1957; Davidson *et al* 1963; Coucowanis *et al* 1975; Seitz *et al* 1975; Venkatalakshmi *et al* 1989). They were all crystallized and dried according to well-established procedures. Single crystals of ^{63}Cu complex doped to extent of 1% and less were made by mixing the corresponding isostructural copper (II) and the diamagnetic host lattice in proper proportions in acetone solutions. These were then slowly evaporated to obtain good single crystals. The morphologies of the crystal were identified with the use of an Enraf-Nonius CAD-4F single crystal diffractometer and an available software.

2.2 Continuous wave method

We used the power saturation method, where the EPR spectra for any possible orientations of the crystal were recorded at several microwave (mw) power levels below saturation. The spin-spin relaxation time, T_2 , has been determined from the line shapes at different mw power levels below saturation. The spin lattice relaxation

time, T_1 , was calculated from the signal amplitudes at different power levels just below saturation, where $\gamma^2 B_1^2 T_1 T_2 \sim 1$. More details on the procedure are found elsewhere (Shimizu 1965; Poole 1967; Brudwig *et al* 1984; Sheila Annie and Manoharan 1992). The power saturation measurements were carried out on a Varian E-112 X-band spectrometer equipped with a TE_{102} cavity for the systems (a) to (d). From the recorded spectra ΔB_{pp} were measured and plotted. Pulsed T_1 measurements were carried out only for crystals (b), (c) and (d).

2.3 Pulse method (inversion recovery)

To avoid spin diffusion, we chose non-selective inversion recovery method (figure 2). A non-selective π pulse is applied for a duration t_p ($100 \mu\text{s}$) to invert the z -magnetization from its equilibrium along the applied magnetic field B_0 . The recovery towards equilibrium is sampled after a delay " t " by a selective $\pi/2$ "detection pulse" that creates transverse magnetization. T_1 is given by

$$M_z(t) = M_0(1 - 2\exp(-t/T_1)), \quad (1)$$

where M_z is the z -magnetization at time t and M_0 is the equilibrium magnetization. The relaxation time T_1 has been determined for the measurements by a three-parameter fit. M_z -values are in arbitrary units and shifted by a constant C caused by the zero line setting of the boxcar averager and has to be added to (1).

The curve-fitting has been done on a Macintosh IIs with the least-square fit program, IGOR, from wave metrics (Lake Oswego, OR 97035, USA). The data have been collected 400ns after the last mw pulse because of the dead time. Every measured curve has 180 data points, independent of the number of Δt steps. All curves have been fitted from data point 33 to eliminate any instrumental artefacts at the beginning. An example of a fitted curve is shown in figure 3.

The regression analysis of the longitudinal relaxation time T_1 as a function of the temperature T has been calculated on a Sun 4 computer with the software package, LAB ONE NMR 1 (New Research Inc. Syracuse, NY 13210). The data points which have been considered for the regression analysis are indicated by circles (figure 4, *vide infra*). The pulse experiments have been carried out at X-band frequency of 9.273 GHz. T_1 measurements have been made on the main Cu hyperfine line having maximum

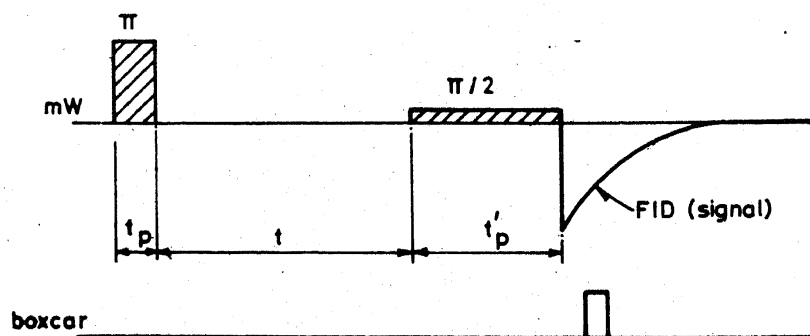


Figure 2. Pulse sequence of the inversion recovery experiment π pulse ($t_p = 100 \mu\text{s}$). $\pi/2$ pulse: ($t'_p = 600 \mu\text{s}$). t is increased in steps of $\Delta t = 5 \mu\text{s}$ to $50 \mu\text{s}$ depending on T_1 . The boxcar averager with an aperture of $15 \mu\text{s}$ is integrating 200 experiments for one t value.

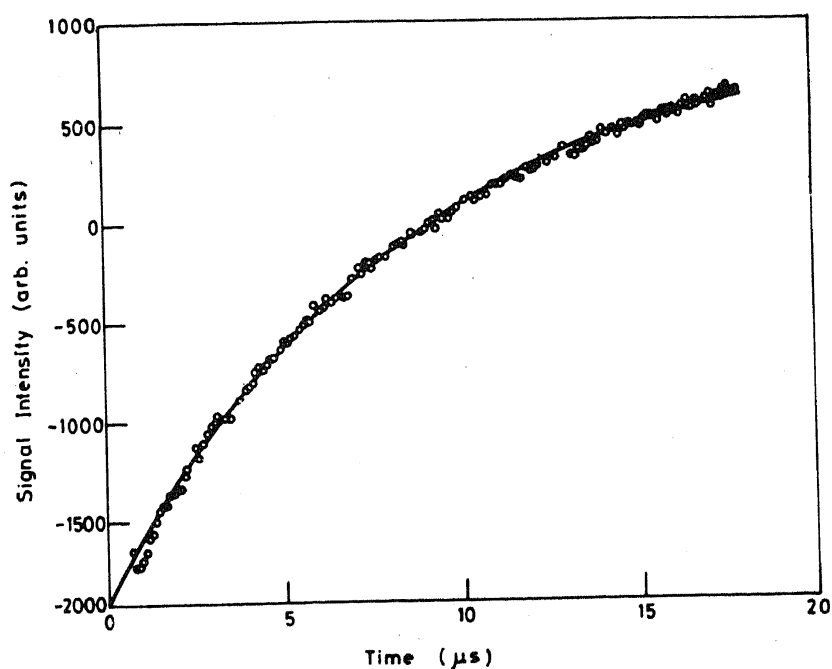


Figure 3. Curve fitting of T_1 measurement on $(n\text{-Bu}_4\text{N})_2(^{63}\text{Cu}/\text{Pd}(\text{dteroc})_2]$ for an arbitrary orientation.

absorption. The forbidden ^{63}Cu hyperfine lines could not be observed in the pulsed EPR because the ratio of the intensity of the forbidden transitions with respect to that of the allowed transitions is very small at the temperatures and orientation chosen for all samples studied.

All pulsed measurements were made with a bridged loop-gap resonator described by Pfenninger *et al* (1988) and a Heli-Tran flow system (Allentown, PA) comprising a transfer line and a quartz dewar to cool the probe head. The temperature has been measured with a calibrated Au(0.07 Fe) chromel thermocouple at the bottom of the resonator.

3. Results and discussion

The temperature-dependent relaxation data obtained for the crystals of matrices (b), (c) and (d) using pulse techniques are presented in figures 4–7. Some of the salient features are summarized as follows.

- (i) The T_1 measurements could be reliably performed with the pulsed methods down to few μs . Therefore, the highest temperature at which T_1 could be measured for each sample was different.
- (ii) There is a slight temperature dependence of T_1 for crystal (c), T_1 data were found to be flat at higher temperatures. A sudden increase in T_1 values on lowering the temperature was observed for crystals (b) and (d), indicating a possible change in the relaxation process. The low temperature T_1 values were of the order of 100 μs and above for (b) and (d), while the value for (c) is only about 10 μs even at the lowest temperature measured. In particular, the values obtained for (b) and (d) comparable to

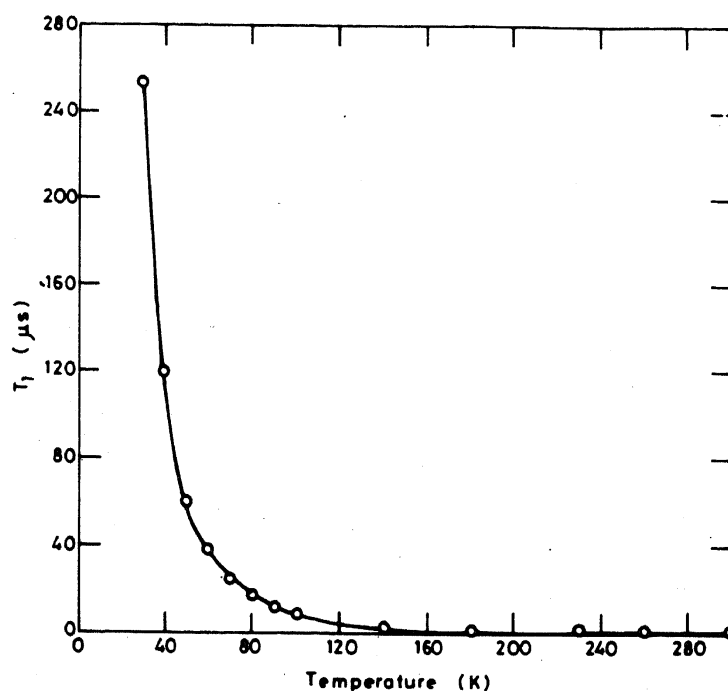


Figure 4. Temperature-dependent T_1 data for $(n\text{-Bu}_4\text{N})_2[{}^{63}\text{Cu/Pt}(\text{dcmdtcroc})_2]$ for $\vec{B} \parallel a$ axis.

those observed for $[\text{Ni(III)/Au(III)}(\text{mnt})_2]^-$ (Kirmse *et al* 1980) as well as the seleno carbamates (Kirmse *et al* 1975).

(iii) At any fixed temperature and orientation $T_1(\text{d}) > T_1(\text{b}) > T_1(\text{c})$.

(iv) As shown in figures 5 and 6, there seems to be an orientation dependence of T_1 in crystal (c) similar to that observed in the case Cu(II)/Zn(II) -bis(diethylselenodithiocarbamates) (Kirmse *et al* 1975). Though the T_1 variations are only about 50% more in $B_\perp(10\bar{3})$ plane (figure 6) compared to B_\perp , (figure 5) the slope of T_1 vs T is the same.

(v) In the echo-detected spectra shown in figure 8 for $(n\text{-Bu}_4\text{N})_2[\text{Cu}(\text{dcmdtcroc})_2]$, the phase memory time is extremely temperature dependent especially for the first two low-field lines and at 120 K most of the lines disappear. But the third line does not show any pronounced temperature dependence, thereby revealing an M_I dependence of the saturation behaviour.

In all these crystals, approximately above 80 K, the T_1 seems to be of the order of a few μs and at temperatures lower than that, there is an enormous increase in T_1 . Under the condition $T \ll \theta_D$ (θ_D is the Debye temperature of solid), the equation (Scott and Jeffries 1962; Abragam and Bleaney 1970),

$$T_1^{-1} = AT + BT^7 + CT^9, \quad (2)$$

is expected to represent the temperature dependent relaxation rate for cupric ions in solid state where A , B and C are constants which include both direct and Raman processes. However, the temperature-dependence of the Raman process for all three systems at high temperature is much weaker than T^9 or T^7 , probably indicating the invalidity of the studied condition $T \ll \theta_D$. A Raman process occurs when a high

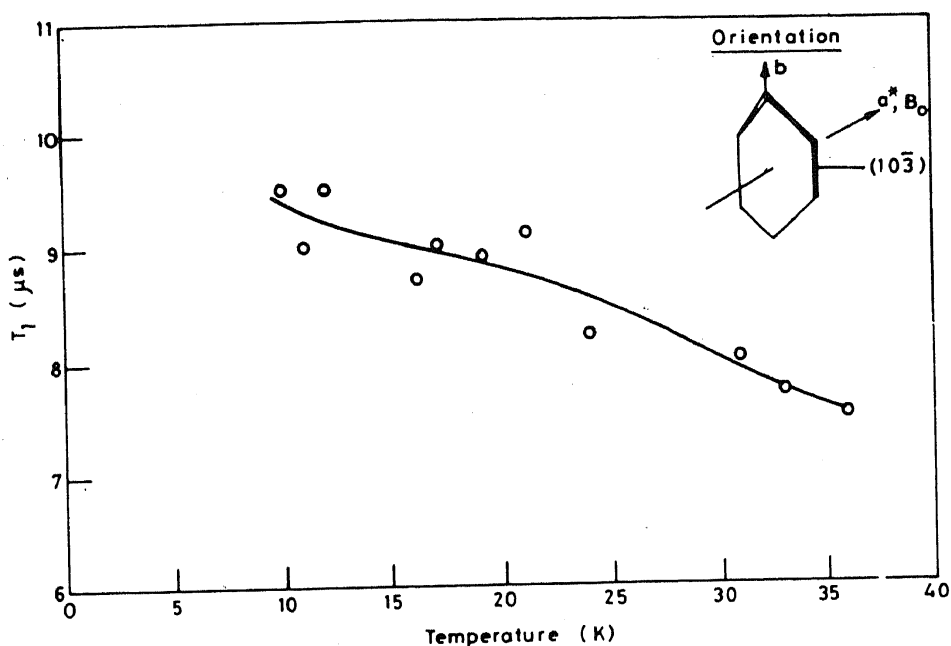


Figure 5. Temperature-dependent T_1 data for $(n\text{-Bu}_4\text{N})_2[{}^{63}\text{Cu}/\text{Pd}(\text{dcmdtroc})_2]$ for $\vec{B} \parallel a$ axis.

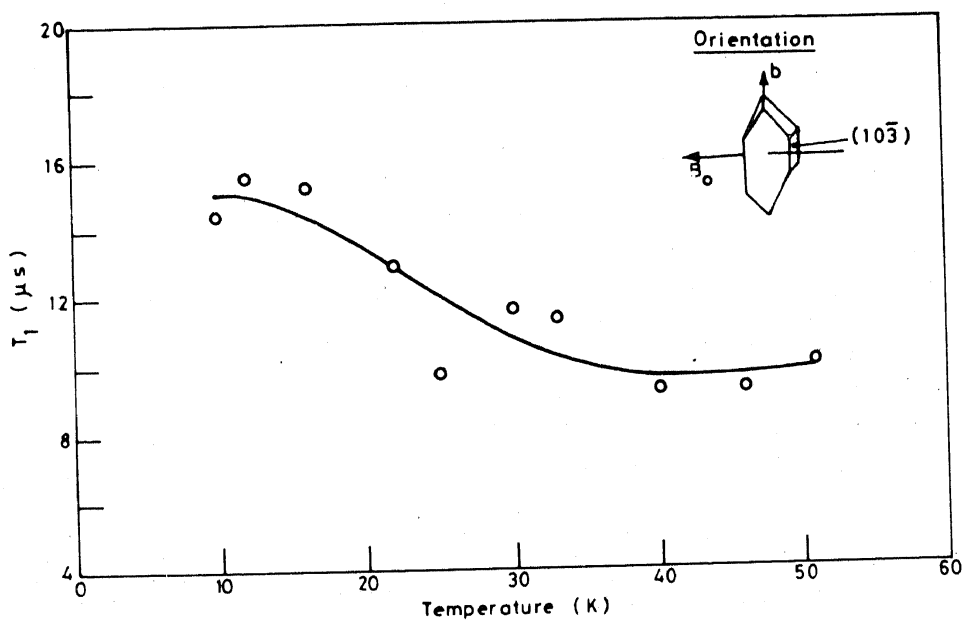


Figure 6. Temperature-dependent T_1 data for $(n\text{-Bu}_4\text{N})_2[{}^{63}\text{Cu}/\text{Pd}(\text{dtroc})_2]$ when $\vec{B} \perp (10\bar{3})$

energy phonon scatters inelastically off a spin and simultaneously flips that spin. The spin-phonon coupling term, B , is large if there are low-lying excited electronic state. The steep increase in T_1 in crystals (b) and (d) at very low temperatures can be interpreted to reveal the existence of direct one-phonon relaxation process. The

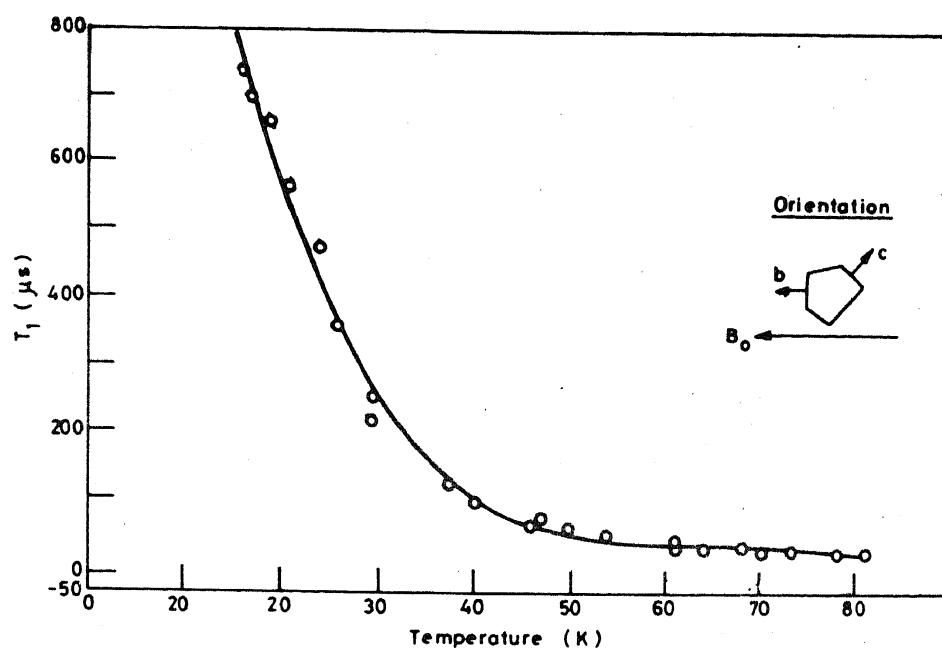


Figure 7. Temperature-dependent T_1 for $(n\text{-Bu}_4\text{N})_2[{}^{63}\text{Cu/Ni}(\text{mnt})_2]$ for $\vec{B}_0 \parallel b$ axis.

observed deviation of T_1^{-1} from T^9 dependence for Raman process as shown in table 1 for systems (b), (c) and (d) can be accounted by introducing a multiplier (Van Vleck 1940; Kurkin *et al* 1972) in the second term of the equation

$$f(\theta_D/T) = J_8(\theta_D/T)/J_8 = \frac{1}{8} \int_0^{\theta_D/T} \frac{x^8 \exp(x) dx}{(\exp(x) - 1)^2} \quad (3)$$

where $x = \hbar\omega/kT$ and ω is the phonon frequency. Similar deviations from $T_1^{-1} \propto T^9$ dependence has been reported earlier (Kirmse *et al* 1974; Aminov *et al* 1976; Solovov and Kirmse 1976) for several copper complexes containing sulphur and seems to be a characteristic feature of these "possibly highly covalent" systems. This also seems to be true of certain blue copper proteins, specially of type variety containing sulphur among ligand atoms (Brudwig *et al* 1984; Scholes *et al* 1984). The comparison of the temperature dependence of T_1^{-1} calculated from (2) and (3) for different values of θ_D with the experimental values allows us to estimate the Debye Temperature, θ_D of these lattices. Using the $f(\theta_D/T)$ values given by Kurkin (Kurkin *et al* 1972) a good agreement between the calculated and measured temperature-dependence of T_1 has been obtained. Thus obtained θ_D values for these different lattices are shown in table 2. These small values for θ_D can be due to strong covalency in the crystals. The θ_D values of 100–300 K in these lattices (b) to (d) compare favourably with 110 K for $\text{Cu(II)/Zn(II)}(\text{dedtc})_2$ (Al'tshuler *et al* 1975), 55–100 K for $[\text{Ni(III)/Au(III)}(\text{mnt})_2]^-$ lattice (Kirmse *et al* 1980) and 70 K for $\text{Cu(II)/Zn(II)}(\text{dedsec})_2$ (Kirmse *et al* 1975).

Using the θ_D values, the average sound velocity $\langle v \rangle$ for the crystals can be estimated (Ho and Ruoff 1967) using the well-known expression,

$$\langle v \rangle = (\theta_D k/h) (3nN\rho/4\pi M)^{-1/3}, \quad (4)$$

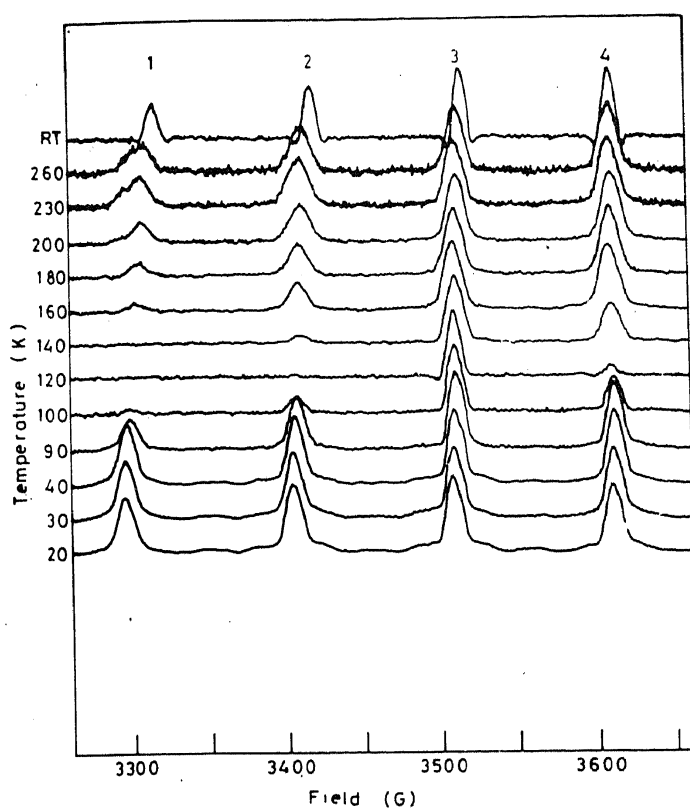


Figure 8. Temperature-dependent echo-detected spectra of $(n\text{-Bu}_4\text{N})_2[{}^{63}\text{Cu}/\text{Pt}(\text{dcmdtroc})_2]$ for $\vec{B} \parallel a$ axis.

where n , M and ρ are respectively the number of atoms in the molecule, molecular weight and the crystal density respectively and others are known parameters. The values for $\langle v \rangle$ are listed in table 2.

At the moment we do not understand why the T_1 values follow the order $T_1(d) > T_1(b) > T_1(c)$ and θ_D follows the order $\theta_D(b) > \theta_D(d) > \theta_D(c)$, the sound velocity following the θ_D order. It is possible that in addition to covalency within a molecule, molecular packing within a unit cell may also play a major part. Another interesting point emerges when we compare the lattices (b), (c) and (d) with at least two more lattices of the similar kind (in terms of covalency) reported earlier (Kirmse *et al* 1975, 1980). This is very much evident in the tables 1 and 2 where such a comparison is made. In all cases, there is a low temperature region for direct process and at high temperatures, $T_1^{-1} \propto T^x$ where x varies from 2.5 to 3.6 in these three crystals. For a Raman process one expects a T^9 or T^7 dependence and hence the observed dependence at higher temperature may be indicative of a possible transition from direct to Raman process as the temperature increases though the contribution of latter process seems to be negligible if one considers a fitting of (2) for all temperatures. Correspondingly, the Debye temperature of solids range from about 70 to 300 K – a low value possible only for highly covalent crystals. At least, it is gratifying to note that all these crystals listed in tables 1 and 2, having similar electronic and bonding properties, display the same order of magnitude with respect to the values of T_1 and θ_D .

Table 1. Temperature dependence of T_1^{-1} for the systems studied.

System in the isostructural diamagnetic lattice	Temperature range (K)	Temperature dependence of T_1^{-1}		Reference
		Low Temp. region	High Temp. region	
$(n - \text{Bu}_4\text{N})_2[\text{Cu}/\text{Pt}(\text{dcm}(\text{dtroc}))_2]$	A: 20-80	$10.8 \times 10^2 T$	$T^{2.57}$	This work
	B: 80-300			This work
	B: 10-51			This work
$(n - \text{Bu}_4\text{N})_2[\text{Cu}/\text{Pd}(\text{dtroc})_2]$	A: 7-30	$1.0 \times 10^2 T$	$T^{2.61}$	This work
	B: 30-90			This work
$(n - \text{Bu}_4\text{N})_2[\text{Cu}/\text{Ni}(\text{mnt})_2]$	A: 2-18	$\{3.2 \times 10^{-6} B^2 + 0.1 [I(I+1) - M_I^2]\} T$	$T^{2.61}$	This work
	B: 18-33			This work
Cu/Zn(dese)				
$(n - \text{Bu}_4\text{N})_2[\text{Ni}/\text{Au}(\text{mnt})_2]$	A: < 9	$1.2 \times 10^2 T$	$0.17 \times 10^{-5} \times f(70/T) T^9$	Kirmse et al (1975)
	B: 9-20			Kirmse et al (1980)

Table 2. Debye temperature (θ_D) and average sound velocity for the systems studied.

System in an isostructural diamagnetic lattice	θ_D (K)	No. of atoms in the molecule (n)	Density (g/cc) (ρ)	Molecular weight (M)	Average sound velocity $\langle v \rangle$ in 10^4 cm/s	Reference
$(n - \text{Bu}_4\text{N})_2[\text{Cu}/\text{Pt}(\text{dcm}(\text{dtroc}))_2]$	298.8	133	1.5	1119	20.45	This work
$(n - \text{Bu}_4\text{N})_2[\text{Cu}/\text{Pd}(\text{dtroc})_2]$	113.0	127	1.24	1023	8.372	This work
$(n - \text{Bu}_4\text{N})_2[\text{Cu}/\text{Ni}(\text{mnt})_2]$	192.0	123	1.4	825	12.86	This work
Cu/Zn(dese)	70.0				5.3	Kirmse et al (1975)
$(n - \text{Bu}_4\text{N})_2[\text{Ni}/\text{Au}(\text{mnt})_2]$	80 ± 20				—	Kirmse et al (1980)

T_1 is different at different orientations as shown in figures 5 and 6 and is due to orientation-dependent contributions. This possibility is probably correct since T_1 versus T slope remains constant for the two studied orientations. A careful temperature and orientation dependence of T_1 made on crystal (d) may throw clear light on the T_1 mechanism. Our results in this case must be considered only as an initial probe into the existence of such a T_1 variation as a function of orientation. To the best of our knowledge, only one such study (Kirmse *et al* 1975) had been conducted earlier and that too for a single plane where again there is only a small increase in T_1^{-1} between two extreme orientations. Even in that report, there was no attempt to rationalize the results.

T_1 values obtained from cw method are presented in table 3 and compared with those from pulse method. As an example the mw power saturation properties of lattice (a) studied at different temperatures are shown in figure 9. Similar results on other lattices are found in another paper (Sheila Annie and Manoharan 1992). Except in the case of crystals (a) and (b), the temperatures at which these measurements were made are above 100 K and compare with "flat response T_1 " from pulse measurements. The T_1 values obtained by cw method are not easily comparable to those by pulse techniques because effective and intrinsic T_1 's are measured respectively. Furthermore, the T_1 values by cw method at high temperatures seem reasonable though the error could be high. The cw method seems to be less sensitive to changes in T_1 with temperature. The long spin-lattice relaxation times are a result of small Debye temperatures and high metal-ligand covalency in these systems. Using the room temperature T_1 values obtained from the cw technique, the line broadening caused by spin lattice relaxation can be calculated with the equation:

$$\Delta B_{SL}[G] = [1.4 \cdot 10^6 \pi g T_1(s)]^{-1}. \quad (5)$$

The line broadening for all the systems studied are given in table 4. Except for system (c) the linewidth contribution from spin-lattice interaction is considerably small and

Table 3. T_1 values from CW saturation studies and corresponding values from pulse method.

System	Temperature (K)	Power (mW)	$\Delta B_{pp}/(\Delta B_{pp})_0$	T_1 (μ s) (from cw saturation)	T_1 (μ s) (from pulse method)
$(n - \text{Bu}_4\text{N})_2[\text{Cu}(\text{dtsq})_2]$	300	100	1.04	0.24	—
	120	100	1.18	0.73	—
	70	100	1.21	0.76	—
$(n - \text{Bu}_4\text{N})_2[\text{Cu}(\text{dcm}(\text{dtroc}))_2]$	300	200	1.17	0.24	0.56
	90	100	1.09	0.49	11.5
	30	50	1.25	—	239.0
$(n - \text{Bu}_4\text{N})_2[\text{Cu}(\text{dtroc})_2]$	300	200	1.03	0.041	—
	120	160	0.95	0.092	—
	30	—	—	—	8.0
	13	—	—	—	9.0
$(n - \text{Bu}_4\text{N})_2[\text{Cu}(\text{mnt})_2]$	300	100	1.06	0.18	—
	120	100	1.16	0.47	—
	60-90	—	—	—	100.0
	30	—	—	—	250.0

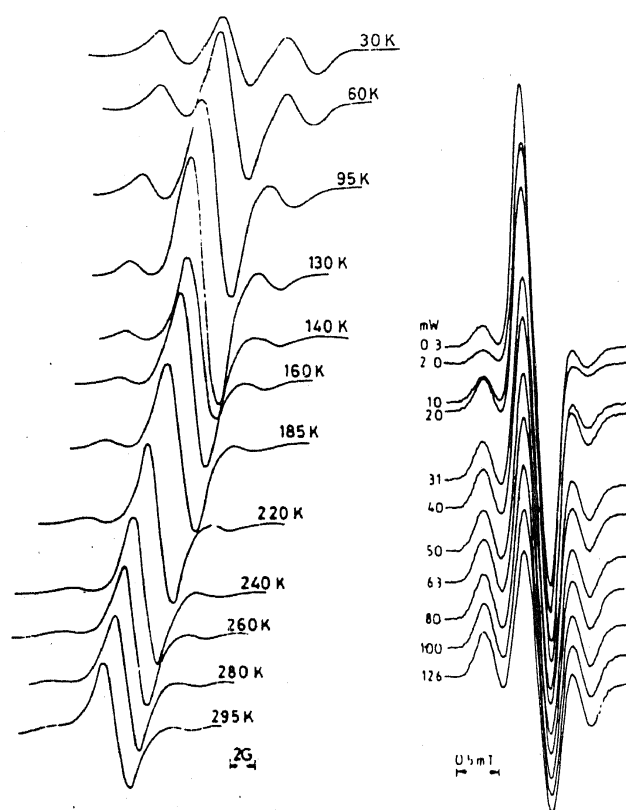


Figure 9. (Left) Temperature-dependence of the high field EPR line due to ^{63}Cu hyperfine interaction and the associated spin-flip transition in $(n\text{-Bu}_4\text{N})_2[\text{Cu}/\text{Pt}(\text{dtsq})_2]$ for $\bar{B} \parallel a$ axis. (Right) Power-dependence of the high field line for the same lattice when $\bar{B} \parallel b$ at 70 K.

Table 4. Linewidth contributions from spin-lattice interactions in some dithiolene anions.

System	$\Delta B_{SL}(\text{G})$	Reference
(a) $(n\text{-Bu}_4\text{N})_2[\text{Cu}(\text{dtsq})_2]$	0.487	This work
(b) $(n\text{-Bu}_4\text{N})_2[\text{Cu}(\text{dcndtcroc})_2]$	0.187	This work
(c) $(n\text{-Bu}_4\text{N})_2[\text{Cu}(\text{dtrroc})_2]$	2.7	This work
(d) $(n\text{-Bu}_4\text{N})_2[\text{Cu}(\text{mnt})_2]$	0.616	This work
(e) $(n\text{-Bu}_4\text{N})_2[\text{Ni}(\text{mnt})_2]$	3.0	Kirmse et al (1980)

accounts for the small linewidth variations as a function of temperature. For system (c) the linewidth is uniformly higher compared to that of the others. Apart from electron spin-lattice relaxation processes the other factors that contribute to linewidth are (1) unresolved ligand hyperfine interactions, (2) and small lattice distortions giving rise to a distribution of the paramagnetic molecules over a small range of orientations and (3) hyperfine interactions caused by protons of the $(n\text{-Bu}_4\text{N})^+$ counter ions. Since the linewidths observed in the single crystal spectra are very small even at room temperature, these other factors have only a limited role – especially the factor (1) is almost absent in these complex ions. Although a quantitative estimate of these

contributions is not feasible, it can be said that linewidth contribution from lattice distortions are small since there is no angular dependence of linewidth but hyperfine interactions from counter-ions should be quite substantial considering the proximity of the (*n*-Bu₄N)-chains at a distance of $\sim 3\text{--}4\text{ \AA}$ to the paramagnetic centre which also give rise to the spin-flip transitions.

For (b) and (d) the relaxation is defined by direct process over a large temperature range. In ionic crystals with other than S-state ions the direct process range is considerably smaller indicating remarkable difference between the phonon spectra of such crystals and that of covalent crystals investigated here. Investigation of spin lattice relaxation in other covalent systems such as organic charge transfer compounds confirm this conclusion (Solovev *et al* 1974). Thus the T_1 data indicates that the extent of covalency should increase as (d) > (b) > (c).

Table 5 lists the T_1 values for crystal (b) for the temperature range from room temperature to 20 K, for all the four copper hyperfine lines. The variations in T_1 values at a given temperature are small and within the range of experimental errors. But at low temperatures where the direct process comes in there is a substantial M_I dependence (Kirmse *et al* 1974) although there is no uniform variation. Specially at low temperatures, T_1 approximately follows the M_I dependent behaviour, i.e., $T_1 = A + BM_I + CM_I^2$. The calculated coefficients A , B and C are also given in the same table 5 along with the T_1 data. Though all coefficients above ~ 80 K have a 'flat response' to temperature a plot of A values (not shown in figure) as a function of temperature gives a curve resembling that of figure 4. Also a plot of coefficients A , B and C as a function of temperature up to 60 K look different from the rest of the temperature regime possibly confirming the presence of direct process as reported in table 1.

Table 5. T_1 data for (*n*-Bu₄N)₂[Cu/Pt(dcmdtcroc)₂] for all four Cu hyperfine lines.

T[K]	T_1 (μ s)				Fitting by M_I dependence ^a		
	$M_I = -3/2$	$-1/2$	$1/2$	$3/2$	A	B	C
300	0.6	0.52	0.54	0.56	0.52	0.10	0.03
260	0.63	0.69	0.7	0.7	0.70	-0.02	-0.02
230	0.9	0.8	0.85	1.2	0.80	-0.10	-0.11
200	1.2	1.1	1.0	1.2	1.03	0.01	0.08
180	1.4	1.2	1.3	1.5	1.23	-0.04	0.10
160	1.6	1.7	1.5	1.9	1.58	-0.07	0.08
140	—	2.6	2.5	2.8	2.53	-0.04	0.09
120	—	—	1.5	4.4	—	—	—
100	8.8	8.7	7.8	7.8	8.24	0.39	0.03
90	12.0	11.0	10.5	11.5	10.62	0.20	0.50
80	17.5	16.0	15.0	15.0	15.41	0.85	0.37
70	25.0	23.5	23.0	23.0	23.96	0.66	0.11
60	38.0	35.0	34.5	35.5	35.50	0.65	0.04
50	60.0	56.0	57.0	64.0	55.80	-0.25	2.76
40	120.0	107.0	103.0	108.0	106.87	4.00	4.50
30	253.0	243.0	195.0	239.0	232.49	8.99	0.01
20	770.0	524.0	433.0	680.0	—(High error)—		

^a Fitting by the equation $T_1 = A + BM_I + CM_I^2$

Similarly we attempted to fit the T_1 values corresponding to each of the M_I values of ^{63}Cu with (3). This gives a very large value for A and a negligible number for B indicating that the dominant mechanism for relaxation is the direct process over the entire temperature region and more particularly so at temperatures ≤ 100 K.

4. Conclusions

In general, the dominant electron spin-lattice relaxation process below 5 K of a Kramer's doublet, say copper ion, is controlled by the direct process. Above about 5 K the dominant mechanism is derived from the Raman process. These observations have been made with many copper complexes. However, in our highly covalent metal dithiolene crystals, the direct process extends over a slightly wider but low temperature region and the contribution of Raman process is felt at higher temperatures. In these crystals, the Raman process can be the dominant relaxation effect at least down to 80 K.

Acknowledgements

One of us (PTM) thanks the Department of Science and Technology, Government of India, for a research grant (SP/S1/F-47/90). Thanks are also due to Dr A Schweiger of ETH, Zurich, Switzerland for helping us in making some measurements at their research laboratory. The data shown in figure 7 were kindly measured for us by Drs P Höfer and D Schmalbein of Bruker Analytische Messtechnik-GmbH, Rheinsteten, FRG.

References

- Abraham A and Bleaney B 1970 *Electron paramagnetic resonance of transition ions* (Oxford: Clarendon)
- Al'tshuler S A, Kirmse R and Solovev B V 1975 *J. Phys.* **C8** 1907
- Aminov L K, Kirmse R and Solovev B V 1976 *Phys. Status Solidi* **77** 505
- Attanasio D, Keijzers C P, van de Berg J P and de Boer E 1976 *Mol. Phys.* **31** 501
- Bahr G and Schleitzer G 1957 *Chem Ber.* **90** 438
- Brudwig G, Blair D F and Chan S I 1984 *J. Biol. Chem.* **259**, 11001, and references therein
- Coucowanis D, Holah D G Hollander F J 1975 *Inorg. Chem.* **14** 2657
- Davidson A, Edelstein N, Holm R H and Maki A H 1963 *Inorg. Chem.* **2** 1227
- Drews A R, Thayer B D, Stapleton H J, Wagner G C, Giugliarelli and Cannistraro S 1990 *Biophys. J.* **57** 157
- Ho P S and Ruoff A L 1967 *Phys. Rev.* **161** 864
- Keijzers C P and Snaathorst D 1980 *Chem. Phys. Lett.* **69** 348
- Kirmse R, Botcher R and Keijzers C P 1982 *Chem. Phys. Lett.* **87** 467
- Kirmse R, Solovev B V and Tarasov B G 1974a *Ann. Phys. (Leipzig)* **31** 352
- Kirmse R, Solovev B V and Tarasov B G 1974b *Fiz. Tverd. Tela.* **16** 1582
- Kirmse R, Solovev B V and Tarasov B G 1975 *Chem. Phys. Lett.* **30** 437
- Kirmse R, Stach J and Botcher R 1980a *Chem. Phys. Lett.* **75** 565
- Kirmse R, Stach J, Dietzsch W and Hoyer E 1978 *Inorg. Chim. Acta* **26** L53
- Kirmse R, Stach J, Dietzsch W, Steimecke G and Hoyer E 1980b *Inorg. Cham.* **19** 2679
- Kurkin I N, Tschirkin Yu K and Shlenkin V I 1972 *Fiz. Tverd. Tela.* **14** 2719
- Mabbs F E and Temperly J 1989 *Spectrochim. Acta* **A45** 285
- Pfenninger S, Forrer J, Schweiger A and Weiland Th 1988 *Rev. Sci. Instrum.* **59** 752

- Poole Jr C P 1967 *Electron spin resonance* (New York: Wiley Interscience)
- Schlick S and Kevan L 1976 *J. Magn. Reson.* **22** 171
- Scholes C P, Janakiraman R, Taylor H and King T E 1984 *Biophys. J.* **46** 1027
- Scott P L and Jeffries C D 1962 *Phys. Rev.* **127** 32
- Seitz G, Mann K and Matusch R 1975 *Arch. Pharm.* **308** 792
- Sheila Annie J and Manoharan P T 1992 *Spectrochim. Acta* **A48** 1715
- Shimuzu H 1965 *J. Chem. Phys.* **42** 3603
- Snaathorst D, Keijzers C P, Klassen A A K, de Boer E, Chaacko V P and Gomperts R 1980 *Mol. Phys.* **40** 585
- Solovev B V and Kirmse R 1976 *Fiz. Tverd. Tela* **18** 3904
- Solovev B V, Kirmse R and Tarasov B G 1974 *Teor. Eksp. Khim.* **10** 413
- Stach J, Kirmse R, Abram U and Dietzsch W 1984a *Polyhedron* **3** 433
- Stach J, Kirmse R and Dietzsch W 1979 *Inorg. Chim. Acta.* **36** L395
- Stach J, Kirmse R, Dietzsch W and Hoyer E 1978 *Inorg. Nucl. Chem. Lett.* **14** 143
- Stach J, Kirmse R, Dietzsch W and Ruth-Maria Olk Hoyer E 1984b *Inorg. Chem.* **23** 4779
- Van Vleck J H 1940 *Phys. Rev.* **57** 426
- Venkatalakshmi N, Varghese B, Lalitha S, Williams R F X and Manoharan P T 1989 *J. Am. Chem. Soc.* **111** 5748